

AE-491

UDC 539.2  
546.289  
543.424

AE-491

## Phonon Anharmonicity of Germanium in the Temperature Range 80-880 K

G. Nelin and G. Nilsson

This report is intended for publication in a periodical. References may not be published prior to such publication without the consent of the author.



AKTIEBOLAGET ATOMENERGI

STUDSVIK, NYKÖPING, SWEDEN 1974



PHONON ANHARMONICITY OF GERMANIUM  
IN THE TEMPERATURE RANGE 80 - 880 K

G Nelin

Royal Institute of Technology, Studsvik, Sweden

and

G Nilsson

Aktiebolaget Atomenergi, Studsvik, Sweden

Phonon frequency shifts and line widths in germanium have been studied in the temperature range 80 - 880 K by means of thermal neutron spectrometry. The results cannot be described in terms of the quasiharmonic approximation in which phonon frequencies are solely volume dependent. Theoretical calculations are found to be more satisfactory for the Raman frequency than for most other modes. A good account of the observed shifts is given by a proposal due to Barron according to which the relative frequency renormalization of a crystal is proportional to the total harmonic vibrational energy. An analysis of the gradients of measured dispersion relations in the principal symmetry directions at 80 K is presented. It is shown that accidental degeneracies may influence the dispersion.

## LIST OF CONTENTS

	<u>Page</u>
I. INTRODUCTION	3
II. EXPERIMENTAL	4
III. RESULTS AND DISCUSSIONS	5
A. Measured Phonon Frequencies	5
B. High-Temperature Frequencies	6
C. Barron's Theory of Frequency Renormalization	7
D. Specific Heat	10
E. Phonon Line Widths	12
IV. ACCIDENTAL DEGENERACIES AND GRADIENTS	13
ACKNOWLEDGEMENT	16
REFERENCE LIST	17
TABLE I	20
TABLE II	21
FIGURE CAPTIONS	22
FIGURES	

## I. INTRODUCTION

Experimental studies of anharmonic effects in crystalline germanium have been reported for specific heat, volume expansion, temperature and pressure dependence of the elastic constants and frequency shift and line broadening of the Raman mode with increase of temperature. These effects are either average properties or long-wave-length limit phenomena. By means of tunnel-junction technique Payne [1] and Zavaritskii [2] observed phonon resonances as functions of pressure at 1 K at the reciprocal point L on the zone boundary. Measurements by the present authors of phonon frequencies all over the Brillouin zone and of line widths for principal symmetry direction modes in germanium at 80 K have been published elsewhere [3, 4]. (Some of these results are illustrated in Fig 3.) Brockhouse and Dasannacharya [5] measured miscellaneous modes at 100 and 700 K and reported observations of frequency shifts.

Few theoretical studies of anharmonicity have been made on germanium and related solids. Dolling and Cowley [6] calculated Grüneisen parameters in germanium assuming only first-neighbour central anharmonic force constants which were determined by a fit to thermal expansion data. Cowley [7] used the same model to generate frequency shifts and widths of the Raman line with rise of temperature. The predicted shifts have subsequently proved to be in good agreement with experimental results. Jex [8] extended the model of Dolling and Cowley to include second-neighbour central interactions. Line widths at 300 K were calculated for the branches  $\Delta_2'$ ,  $\Delta_5(A)$  and  $\Lambda_3(A)$  together with some frequency shifts for the  $\Delta$ -branches. The results show a considerable frequency renormalization for transverse acoustic modes around the zone

boundary. The characteristic difference between diamond and germanium as regards the dispersion of these branches should thus to a great part be due to anharmonic effects. Subsequently, Jex [9] has reported calculations of phonon line widths at 80 K for all branches in the principal symmetry directions. These results are in fair agreement with experiment [3] except for the acoustic branch  $\Sigma_3(A)$ , in which case there is a considerable discrepancy.

In the present paper we present experimental results of frequency shifts and line widths for phonon modes at  $\Gamma$ , X and L in germanium in the temperature range 80 - 880 K. The data are also analysed and compared with other theoretical and experimental results.

## II. EXPERIMENTAL

The present experiment was carried out using a double-monochromator crystal spectrometer [10] and the 50 MW research reactor R2 at Studsvik. In most respects the procedures adopted and the resolutions applied were identical with those described in Ref [3]. Optic modes were, however, not observed with a resolution as good as that previously obtained because the monochromator of the present instrument were restricted to Cu (220) reflections. (In the previous work (420) reflections were also available.) Typical figures for the energy resolution of optic modes were 0.30 - 0.40 THz for modes with vanishing frequency gradients. This had, however, an almost negligible influence on the accuracy of the recorded frequencies of the modes considered in the present work.

The intrinsic phonon line widths of germanium are small and in consequence their extraction from the observed peak widths requires very good counting statistics. At temperatures above

300 K this requirement was not fulfilled except for transverse acoustic modes.

The germanium crystal was one third the size of that used in Ref [3] and from which it was cut. The crystal was mounted in a thermostat shielded so effectively as to limit temperature variations at the sample to a few degrees at 800 K.

### III. RESULTS AND DISCUSSIONS

#### A. Measured Phonon Frequencies

The modes studied were those of the symmetry points  $\Gamma$ , X and L. These are associated with most of the characteristic features of the phonon density of states spectrum [4] and they are accordingly significant for all phenomena dependent upon one- or two-phonon densities, such as, e.g., infra-red absorption. The present results are plotted in Fig 1. Brockhouse and Dasannacharya [5] found that the relative frequency shifts accompanying a change of temperature were approximately constant for all modes considered. This does not apply to the results obtained in the present work, where the relative shifts may vary by as much as one third about their mean value. The actual values are  $-0.53(\Gamma'_{25})$ ,  $-0.54(L'_3)$ ,  $-0.52(L_1)$ ,  $-0.43(L'_2)$ ,  $-0.82(L_3)$ ,  $-0.75(X_4)$ ,  $-0.47(X_1)$  and  $-0.86(X_3)$  when expressed as percent per 100 degrees. By means of tunnel-junction technique Payne [1] and Zavaritskii [2] observed phonon resonances in germanium at 1 K at the reciprocal point L and in the latter work even at  $\Gamma$ . The results are in fair agreement with those obtained at 80 K in the present experiment. The temperature dependence of the Raman active mode  $\Gamma'_{25}$  has been studied by Cerdeira and Cardona [11] and by Ray et al. [12]. The results of the present work are in best agreement with the formers' data and also with those of a previous

Raman scattering experiment by Parker et al. [13], who reported the value 9.015 THz at 300 K (not shown in Fig 1).

### B. High-Temperature Frequencies

The frequency  $\nu_{\tilde{q}j}$  of a vibrational mode is in the general theory a function of the mutually dependent thermodynamic variables  $P$ ,  $V$  and  $T$ . We may write

$$\left(\frac{\partial \nu_{\tilde{q}j}}{\partial T}\right)_P = \left(\frac{\partial \nu_{\tilde{q}j}}{\partial T}\right)_V + \left(\frac{\partial \nu_{\tilde{q}j}}{\partial V}\right)_T \left(\frac{\partial V}{\partial T}\right)_P. \quad (1)$$

In the harmonic approximation  $\nu_{\tilde{q}j}$  is independent of  $T$ . The volume does vary with temperature, however, and in the so-called quasi-harmonic approximation  $\nu_{\tilde{q}j}$  is allowed to change with volume while interaction between different modes is considered to be negligibly small. Thus  $\left(\frac{\partial \nu_{\tilde{q}j}}{\partial T}\right)_V$  is a purely anharmonic term. The variation of  $\nu_{\tilde{q}j}(V(T))$  has been calculated in the quasiharmonic approximation using the deformation dipole model developed by Tolpygo [14]. (The lattice constant data were taken from Carr et al. [15] and from Gibbons [16] in the ranges 8 - 130 K and 130 - 300 K, respectively. Above 300 K the required values were obtained by extrapolation from Gibbons' data employing a fitted third degree polynomial.) The results, normalized with respect to the present data at 80 K, are presented as dashed lines in Fig 1. They show that the major part of the frequency shift is, according to Tolpygo's model, due to purely anharmonic effects. (A check of the accuracy of the calculated quasiharmonic frequencies is given in Sec III D.)

By definition

$$\beta = 3\alpha = (1/V)\left(\frac{\partial V}{\partial T}\right)_P \quad \text{and} \quad \kappa = -(1/V)\left(\frac{\partial V}{\partial P}\right)_T, \quad (2)$$

where  $\alpha$  is the linear coefficient of thermal expansion and  $\kappa$  the isothermal compressibility. Eqs (1) and (2) give

$$\tilde{(\partial v_{qj}/\partial T)}_P = \tilde{(\partial v_{qj}/\partial T)}_V - (3\alpha/\kappa) \tilde{(\partial v_{qj}/\partial P)}_T, \quad (3)$$

where  $\alpha$  and  $\kappa$  relate to the appropriate values of  $P$ ,  $V$  and  $T$ . Inspection of Fig 1 reveals that  $\tilde{(\partial v_{qj}/\partial T)}_{P=0}$  is, within the limits of experimental error, a constant at higher temperatures. The quasiharmonic derivatives,  $\tilde{(\partial v_{qj}/\partial T)}_{P=0}^{q-h}$ , seem not to be quite constant in this region but let us assume they are so. The anharmonic contribution  $\tilde{(\partial v_{qj}/\partial T)}_V$  can then be obtained either from Eq (1) via the identification  $\tilde{(\partial v_{qj}/\partial T)}_P^{q-h} = \tilde{(\partial v_{qj}/\partial V)}_T \tilde{(\partial V/\partial T)}_P$  or, if  $\tilde{(\partial v_{qj}/\partial P)}_T$  is known, from Eq (3). Zavaritskii [2] measured  $\tilde{(\partial v_{qj}/\partial P)}_{T=1K}$  for  $\Gamma'_{25}$  and the modes at L under hydrostatic pressure. These derivatives, which were found to be independent of  $P$ , are applicable only if it is assumed they are constant in  $T$ . Table I demonstrates, however, that clear differences exist between  $\tilde{(\partial v_{qj}/\partial T)}_{P=0}^{q-h}$  and  $(-3\alpha/\kappa) \tilde{(\partial v_{qj}/\partial P)}_{T=1}^{Zav}$ . (The compressibility data needed were taken from McSkimin [17]). An experimental check would probably reveal that the assumption of temperature independence for  $\tilde{(\partial v_{qj}/\partial P)}_T$  is invalid. It would be particularly interesting to check the postulated change of sign of this quantity for the mode  $L_3$  between the low and the high temperature region.

Finally, columns II and V in Table I show that the frequency shifts with temperature due to volume expansion are constant, provided they are expressed in the form  $\tilde{(\partial v_{qj}/\partial T)}_P/v_{qj}$ , while the  $\tilde{(\partial v_{qj}/\partial T)}_V/v_{qj}$  for the purely anharmonic effects vary by a factor of three between the smallest and the largest value.

### C. Barron's Theory of Frequency Renormalization

Barron [18] proposed that the frequency renormalizations might be evaluated by assuming the relative shifts to be proportional to the harmonic vibrational energy of the crystal, i. e.  $\partial v/v = A \langle E_{vib}^h \rangle$ .

This may be written

$$\tilde{\nu}_{\tilde{qj}}(T) = \tilde{\nu}_{\tilde{qj}}^h \left[ 1 + \frac{1}{3Nk\theta_{\tilde{qj}}} \left\langle \sum_{\tilde{qj}} h \nu_{\tilde{qj}}^h \left( n_{\tilde{qj}} + \frac{1}{2} \right) \right\rangle \right], \quad (4)$$

where  $\tilde{\nu}_{\tilde{qj}}^h$  is the harmonic frequency and  $n_{\tilde{qj}}$  is its Bose-Einstein distribution function. Barron's constant A, usually assumed to be identical for all modes, has been redefined to include a temperature,  $\theta_{\tilde{qj}}$ , characteristic of each mode. Feldman et al. [19] showed that for the nearest-neighbour central-force model Barron's proposal leads to an exact expression for the frequency shift due to the quartic term in the expansion of the lattice potential energy. The contributions from the cubic term were found to be exactly described in the high and low temperature limits. It is known that in a solid such as germanium bond-stretching forces between nearest-neighbours dominate the interactions. Eq (4) should thus be expected to yield a good first approximation for most of the frequency renormalizations. Barron [18] also pointed out that a shift obtained from neutron scattering is the same as that obtained from the entropy but not to that obtained from the free energy. Although this relationship is not exact, as was shown by Horton [20], the discrepancy is probably negligible for weakly anharmonic crystals like germanium. Thus the average vibrational energy in Eq (4) may in the present case be replaced by  $3Nh\nu_g \left( n_g + \frac{1}{2} \right)$ , where  $\nu_g$  is the geometric mean frequency associated with the entropy.  $\nu_g$  has been determined to  $(5.110 \pm 0.015)$  THz from specific heat data by Flubacher et al. [21] and the value 5.11 THz was obtained from neutron scattering data [4]. Eq 4 then reads

$$\tilde{\nu}_{\tilde{qj}}(T) = \tilde{\nu}_{\tilde{qj}}^h \left[ 1 + \frac{h\nu_g}{k\theta_{\tilde{qj}}} \left( \frac{1}{e^{h\nu_g/kT} - 1} + \frac{1}{2} \right) \right] \quad (5)$$

giving an absolute zero frequency of

$$\tilde{\nu}_{\tilde{qj}}^h(0) = \tilde{\nu}_{\tilde{qj}}^h \left[ 1 + \frac{h\nu_g}{2k\theta_{\tilde{qj}}} \right]. \quad (6)$$

A fit of Eq (5) to the present data by the method of least squares with  $\tilde{\nu}_{\tilde{qj}}^h$  and  $\theta_{\tilde{qj}}$  as free parameters, presented in Fig 1 and Table II, is found to be good. The data at 80 K are close to the harmonic spectrum. The  $\tilde{\nu}_{\tilde{qj}}^h(0)$ 's lie within the limits of experimental error, while the  $\tilde{\nu}_{\tilde{qj}}^h$ 's exceed the error limits by 0.03 THz, or 0.6% of  $\nu_g$  on the average. The contributions to the frequency shifts from the cubic and the quartic terms in the expansion of the lattice potential are of opposite sign [22]. The negative values obtained for the  $\theta_{\tilde{qj}}$ 's show that the cubic terms dominate. It is also noteworthy that these values are of the same magnitude as those characteristic of the temperatures corresponding to the energy differences between the lowest conduction and the highest valence band levels [23].

Cowley [7] calculated the renormalization of  $\Gamma'_{25}$  assuming nearest-neighbour central interactions and contributions only from third order terms in the lattice potential. His results, normalized to 9.01 THz at 300 K, are represented in Fig 1 by open circles. The temperature dependence is somewhat stronger than that found in the present work but still within the limits of error. The renormalization at absolute zero, roughly -0.05 THz, is close to the present value of  $-(0.06 \pm 0.02)$  THz. Jex [8] extended Cowley's model to include central forces with second-nearest neighbours. His frequency-dependent renormalizations for the transverse acoustic branches  $\Delta_5(A)$  and  $\Lambda_3(A)$  amount to roughly 10% at the zone boundary. The renormalizations of the remaining  $\Delta$ - and  $\Lambda$ -branches gave values which are one order of magnitude lower. The latter result is in fair agreement with the present findings while the former is in sharp contrast.

### D. Specific Heat

The specific heat at constant and vanishing pressure is given by the relationship [24]

$$C_P = T(\partial S/\partial T)_P. \quad (7)$$

If the phonon system is assumed to be weakly interacting it may be approximated to an ideal Bose gas. This yields the entropy [24]

$$S = k \sum_{\mathbf{x}} \{x/(e^x - 1) - \ln(1 - e^{-x})\}; \quad x = h\nu_{\mathbf{qj}}(T)/kT. \quad (8)$$

Equations (5) and (6) may be written

$$\nu_{\mathbf{qj}}(T) = \nu_{\mathbf{qj}}(0) F(T); \quad F(T) = [1 + \gamma/(\exp(h\nu_g/kT) - 1)] \quad (9)$$

In Eq (9) it is assumed that all modes are subject to the same percental frequency shift with temperature. The actual value  $\gamma = -1.385 \times 10^{-2}$  is obtained from the mean value of  $\theta_{\mathbf{qj}}$  in Table II. Standard procedures then yield

$$C_P = 3Nk \int_0^{\nu_{\max}} (y^2 \sinh^{-2} y) g(\nu) d\nu \left\{ 1 - \frac{F'(T)}{F(T)} T \right\};$$

$$y = h\nu F(T)/2kTF(80). \quad (10)$$

The frequencies and the densities of states are those obtained at 80 K [3, 4]. The "harmonic" specific heat  $C_V^h$  (including the zero points motions) is obtained from  $C_P$  by setting  $F(T) = F(80)$  and omitting the expression within the braces.

Figure 2a shows the results of the present calculation of  $C_P$  and  $C_V^h$  together with experimental data. The agreement of  $C_P$  with the well established data of Piesbergen [26] and Flubacher et al. [21] and of  $C_V^h$  with the constant of Dulong and Petit as well is good. The

results of Greiner [27], Smith [28] and Gerlich et al. [29] receive little support from the low-temperature data. The differences between the "best" specific heat data and  $C_V^h$  is plotted in Fig 2b together with the present values for  $C_P - C_V^h$ . If the results of Piesbergen were correct an error of about 80% is inferred for the present value of  $\Delta C_P^a$  at 270 K. The anharmonic contributions extracted from the data by Chen and Turnbull [25] exhibit smaller percental deviations from the present results than those of Piesbergen but they have a strange shape as can be seen even from Fig 2a. The deviations from the data of Flubacher et al. are considerably smaller and, moreover, these authors performed a calculation of  $C_V^h$  up to 300 K which gave results in excellent agreement with the present values of  $C_V^h$ . A definite statement of how well the mean frequency shift of the symmetry point phonon modes represent the mean of all modes must, however, await more accurate high temperature specific heat data.

Due to volume expansion the specific receives a contribution [24]

$$C_P - C_V = \beta^2 T v / \kappa , \quad (11)$$

where  $v$  is the molar volume. At 300 K,  $C_P - C_V = 2.3 \times 10^{-2}$  cal/g-at deg), while the corresponding value obtained from the quasiharmonic shifts of the present study (see Sec IIIB) is  $1.6 \times 10^{-2}$  cal/g-at deg). The difference is 7% of the total anharmonic contribution,  $\Delta C_P^a$ , and the errors of the calculated quasiharmonic shifts should therefore have no influence on the conclusions drawn in Sec IIIB.

### E. Phonon Line Widths

A very striking feature of the present results is the lack of an evident broadening of the peak widths with temperature for the transverse acoustic modes  $X_3$  and  $L_3$ . The widths observed only slightly exceed the calculated resolution widths. More noteworthy, however, is the fact that even the observed widths are smaller than theoretically estimated line width values. (It should be remembered that an observed peak is a convolution of the resolution function with the neutron cross section (phonon line).). At 300 K, for instance, Jex [8] predicts a line width of 0.23 THz for  $L_3$ , while the width of the observed peak is  $(0.13 \pm 0.01)$  THz. In the high temperature limit, the line widths are expected to vary approximately linearly with temperature. Then, if scaled to 700 K, the values of Jex would read 0.30 THz for  $X_3$  and 0.54 THz for  $L_3$ , while we have recorded  $(0.13 \pm 0.01)$  and  $(0.12 \pm 0.01)$  THz, respectively. We believe the phonon line widths of these modes not to exceed a few units of 0.01 THz anywhere in the temperature region covered.

The rest of the modes considered were not very suitable for line width studies as a function of temperature because of insufficient counting statistics and, at the highest temperatures, multiphonon contributions and incoherent processes that interfered with the one-phonon resonances.

The valence-force-field model seems to be the best existing harmonic approximation to the lattice dynamics of germanium [30, 31]. This model is founded on bond-stretching and angle-bending forces and interactions between them. The former are central two-body forces which operate between nearest-neighbours and the latter are three-body forces which act between first and second-nearest neighbours. In this theory the dynamics of transverse

acoustic branches are dominated by the angle-bending forces and the zone boundary modes  $L_3$  and  $X_3$  are entirely governed by them. Angular forces were not included in the calculations by Jex. It is possible that omission of angular forces may lead to erroneous results for transverse acoustic branches.

#### IV. ACCIDENTAL DEGENERACIES AND GRADIENTS

Kagan and Zhernov [32] used the Green's function method to analyse the influence of anharmonicity on phonon dispersion near a point of accidental degeneracy. It was found that modes involved in such a degeneracy may have different renormalizations and life-times. Even when branches come close to one another, without actually intersecting, they should influence each other significantly. An observation of the removal of an accidental degeneracy may lie beyond the possibilities of present day neutron physics. However, according to Kagan and Zhernov even matrix elements belonging to wave vectors close to the one under consideration are affected by the anharmonicity so that anomalies or "kinks" are to be expected in the dispersion relations. Such effects are likely to be more easily observed than a removal of degeneracy. Cowley [33] has questioned the validity of the conjecture of Kagan and Zhernov. From a group theoretical point of view it is difficult to understand why a perturbation with the same symmetry as the crystal should cause a coupling between phonons belonging to different irreducible representations. In fact, Kagan and Zhernov tacitly assumed the existence of non-diagonal elements with this property. The symmetry properties of the phonon propagator for an arbitrary crystal have actually been studied by Maradudin and Ipatova [34]. Their work shows that non-vanishing off-diagonal elements only cause a

coupling between solutions of specific modes. These are modes which polarization vectors transform according to the same irreducible representation.

In the case of germanium at 80 K an inspection of Figs 3 and 4 reveals the following:

- i) The wave vector of the accidental degeneracy between the branches  $\Delta'_2$  and  $\Delta_5(0)$  is marked by the symbol  $q_1$  in Figs 3, 4a and 4b. Pronounced kinks are observed at  $q_1$  in the gradients of the well separated branches  $\Delta'_2$  and  $\Delta_1$ . Within the limits of error, no kinks are clearly visible in the velocity curves for  $\Delta_5(A)$  and  $\Delta_5(0)$ , but they have a change in slope around  $q_1$ .
- ii)  $q_2$  marks the wave vector below which the two branches  $\Lambda_1(0)$  and  $\Lambda_3(0)$  could not be resolved. When a region of close contact is that extended it is difficult to separate surmised anomalies from the general behaviour of the curves (see Figs 4c and 4d). However, the velocity curve of the well separated branch  $\Lambda_1(A)$  obviously possesses irregularities in the region considered. It is to be noted that the irreducible representation  $\Lambda_1$  corresponds to the same phonon polarizations as  $\Delta_1$  and  $\Delta'_2$ , namely the linearly longitudinal mode. The representations  $\Lambda_3$  and  $\Delta_5$  are associated with the linearly transverse mode of polarization.
- iii) Another region of close contact between two branches is afforded by  $\Sigma_1(A)$  and  $\Sigma_3(0)$ . The symbol  $q_3$  indicates the wave vector of minimum frequency for the branch  $\Sigma_3(0)$ . When passing through  $q_3$  the slope of the velocity curve changes for both  $\Sigma_1(A)$  and  $\Sigma_3(0)$ . The same effect is observed for all  $\Sigma$ -branches except,

maybe,  $\Sigma_3(A)$ . The larger scattering of points around  $q_3$  in Fig 4 than elsewhere originates from the fact that phonon frequencies were determined for a more dense selection of wave vectors in this region.

- iv) The last region of interest in Fig 3 is that marked by  $q_4$  at the point of accidental degeneracy between the elliptically polarized branch  $\Sigma_1(0)$  and the linearly transverse  $\Sigma_2$ . (All other branches are elliptically polarized, except that of  $\Sigma_4$  which is linearly transverse.) Figures 4e - g exhibit nothing irregular at  $q_4$  with the possible exception of the branch  $\Sigma_4$ .
- v) Figure 4a shows an unexpected dip, marked  $q_5$ . Its origin may, perhaps, be connected with the fact that  $q_5$  coincides with the minimum of the velocity curve of  $\Delta_5(0)$  (see Fig 4b). As seen from Fig 3, however, nothing noteworthy is present in any of the branches at  $q_5$ .

A nine-parameter version of the deformation dipole model [35], which is equivalent to the shell model [36], affords an excellent fit to the  $\Delta$ - and the  $\Lambda$ -branches of germanium at 80 K. This fit is even somewhat better than that of the valence-force-field model [31]. If the  $\Sigma$ -direction is included, however, the good fit is lost. The velocity curves of the  $\Delta$ - and the  $\Lambda$ -branches as obtained from this fit are represented by solid lines in Figs 4a - d. The kinks observed in the experimental results are obviously not compatible with this model.

In conclusion, the present analysis does not prove that the irregularities observed in the phonon gradients are of anharmonic origin. It indicates, however, that an accidental degeneracy or a close approach between branches may well influence the dispersion.

The observed irregularities may also be explained on the basis of a more sophisticated harmonic model or in terms of a perturbation which does not share the crystal symmetry.

#### ACKNOWLEDGEMENT

We are indebted to Dr L Bohlin for illuminating discussions on the problems dealt with in Sec IV.

REFERENCE LIST

1. Payne, R T,  
Shift of [111] Phonon Energies at the Brillouin Zone  
Boundary under Uniaxial Stress in Germanium,  
Phys Rev Letters, 13(1964) p 53
2. Zavaritskii, N V,  
Shift of singularities of Germanium lattice vibration  
spectrum under pressure,  
Sov Phys JETP Letters 12(1970) p 18
3. Nilsson, G and Nelin, G,  
Phonon Dispersion Relations in Ge at 80°K,  
Phys Rev B3(1971) p 364
4. Nelin, G and Nilsson, G,  
Phonon density of states in Germanium at 80 K measured  
by neutron spectrometry,  
Phys Rev B5(1972) p 3151
5. Brockhouse, B N and Dasannacharya, B A,  
Temperature Effects on Lattice Vibrations in Germanium,  
Solid State Commun 1 (1963) p 205
6. Dolling, G and Cowley, R A,  
The thermodynamic and optical properties of germanium,  
silicon, diamond and gallium arsenide,  
Proc Phys Soc 88(1966) p 463
7. Cowley, R A,  
Raman scattering from crystals of the diamond structure,  
J Phys (Paris) 26(1965) p 659
8. Jex, H,  
Anharmonic interactions in diamond-type crystals,  
Phys Stat Sol (b) 45 (1971) p 343
9. Jex, H,  
Phonon Lifetimes in Germanium,  
Physics Letters 41A(1972) p 79
10. Stedman, R, Almqvist, L, Raunio, G and Nilsson, G,  
New Crystal Spectrometer for Neutrons,  
Rev Sci Instr 40(1969) p 249
11. Cerdeira, F and Cardona, M,  
Effect of carrier concentration on the Raman frequencies of  
Si and Ge,  
Phys Rev B5(1972) p 1440
12. Ray, R K, Aggarwal, R L and Lax, B,  
Temperature dependence of Raman scattering in Germanium,  
Proc of the 2nd international conference on light scattering  
in solids, Paris 19 - 23 Jul 1971, p 288
13. Parker, J H Jr, Feldman, D W and Ashkin, M,  
Raman Scattering by Silicon and Germanium,  
Phys Rev 155(1967) p 712

14. Tolpygo, K B,  
Long-range Forces and the Dynamical Equations for Homopolar Crystals of the Diamond Type,  
Sov Phys Solid State 3(1961) p 685
15. Carr, R H, McCammon, R D and White, G K,  
Thermal Expansion of Germanium and Silicon at low Temperatures,  
Phil Mag 12(1965) p 157
16. Gibbons, D F,  
Thermal Expansion of Some Crystals with the Diamond Structure,  
Phys Rev 112(1958) p 136
17. McSkimin, H J,  
Measurement of Elastic Constants at Low Temperatures by Means of Ultrasonic Waves - Data for Silicon and Germanium Single Crystals, and for Fused Silica,  
J Appl Phys 24(1953) p 988
18. Barron, T H K,  
Thermodynamic properties and effective vibrational spectra of an anharmonic crystal in lattice dynamics,  
Proc of intern conf, Copenhagen,  
Pergamon Press Inc, New York 1965, p 247
19. Feldman, J L, Horton, G K and Lurie, J B,  
A one-parameter treatment of anharmonic specific heat,  
J Phys Chem Solids 26(1965) p 1507
20. Horton, G K,  
Ideal Rare-Gas Crystals,  
Am J Phys 36(1968) p 93
21. Flubacher, P, Leadbetter, A J and Morrison, J A,  
The Heat Capacity of Pure Silicon and Germanium and Properties of their Vibrational Frequency Spectra,  
Phil Mag 4(1959) p 273
22. Leibfried, G and Ludwig, W,  
Theory of anharmonic effects in crystals,  
Solid State Phys 12(1961) p 275
23. Cohen, M L and Bergstresser, T K,  
Band Structures and Pseudopotential Form Factors for Fourteen Semiconductors of the Diamond and Zinc-blende Structures,  
Phys Rev 141(1966) p 789
24. Huang, K,  
Statistical Mechanics,  
John Wiley & Sons, Inc, New York 1963
25. Chen, H S and Turnbull, D,  
Specific Heat and Heat of Crystallization of Amorphous Germanium,  
J Appl Phys 40(1969) p 4214

26. Piesbergen, U,  
The mean atomic heats of the III - V semiconductors  
AlSb, GaAs, InP, InAs and InSb and the element Ge  
between 12 and 273°K,  
Z Naturforsch 18A(1963) p 141
27. Greiner, E S,  
Specific Heat, Latent Heat of Fusion and Melting Point  
of Germanium,  
J Metals 4(1952) p 1044
28. Smith, R C,  
High-Temperature Specific Heat of Germanium,  
J Appl Phys 37(1966) p 4860
29. Gerlich, D, Abeles, B and Miller, R E,  
High-Temperature Specific Heats of Ge, Si and Ge-Si  
Alloys,  
J Appl Phys 36(1965) p 76
30. Solbrig, A W Jr,  
Valence Force Potentials for Calculating Crystal Vibrations  
in Silicon,  
J Phys Chem Solids 32(1971) p 1761
31. Nilsson, G and Nelin, G,  
Study of the homology between Silicon and Germanium by  
thermal-neutron spectrometry,  
Phys Rev B6(1972) p 3777
32. Kagan, Yu and Zhernov, A P,  
Effect of anharmonicity on the phonon spectrum near a point  
of degeneracy,  
Sov Phys JETP 21(1965) p 646
33. Caglioti, G et al. ,  
Neutron inelastic scattering. Proc of a symposium, Copen-  
hagen,  
Vienna 1968. Discussion, Vol 1, p 378
34. Maradudin, A A and Ipatova, I P,  
Structure of the phonon propagator for an anharmonic  
crystal,  
J Math Phys 9(1968) p 525
35. Demidenko, Z A, Kucher, T I and Tolpygo, K B,  
Characteristic frequencies of germanium lattice vibrations  
calculated in various approximations,  
Sov Phys Solid State 3(1962) p 1803
36. Cochran, W,  
Theory of the lattice vibrations of germanium,  
Proc Roy Soc A253(1959) p 260

TABLE I

High-temperature phonon-frequency derivatives in units of  $10^8 \text{ K}^{-1} \text{ sec}^{-1}$  for the modes studied in the present work. I) Values obtained by least-squares fits of straight lines to the data in Fig 1 above 80 K. II) Ditto from the quasiharmonic approximation as described in the text. III) Values obtained by Zavaritskii [2] and from high-temperature lattice expansivity and compressibility data. IV) The purely anharmonic contributions as obtained by means of Eq (3) and Columns I and III. V) Ditto from Eq (1) and columns I and II. The figures listed within parantheses in columns II, IV and V are the absolute values of the ratios between the various derivatives and the frequencies in units of  $10^{-4} \text{ K}^{-1}$ .

mode	$(\partial \nu_{\tilde{q}j} / \partial T)_{P=0}$		$(-3\alpha/\kappa)(\partial \nu_{\tilde{q}j} / \partial P)_{T=1}$	$(\partial \nu_{\tilde{q}j} / \partial T)_V$	
	I	II	III	IV	V
$\Gamma'_{25}$	$-4.7 \pm 0.4$	-1.3 (0.15)	$-2.0 \pm 0.1$	$-2.7 \pm 0.5$ (0.30)	$-3.4 \pm 0.4$ (0.38)
$L'_3$	$-4.6 \pm 0.6$	-1.2 (0.14)	$-2.0 \pm 0.1$	$-2.6 \pm 0.7$ (0.31)	$-3.4 \pm 0.6$ (0.40)
$L_1$	$-3.7 \pm 0.4$	-1.0 (0.14)	$-2.2 \pm 0.1$	$-1.5 \pm 0.5$ (0.21)	$-2.7 \pm 0.4$ (0.38)
$L'_2$	$-2.8 \pm 0.4$	-0.96 (0.15)	$-0.5 \pm 0.1$	$-2.3 \pm 0.5$ (0.35)	$-1.8 \pm 0.4$ (0.26)
$L_3$	$-1.5 \pm 0.3$	-0.27 (0.15)	$+0.6 \pm 0.1$	$-2.1 \pm 0.4$ (1.15)	$-1.2 \pm 0.3$ (0.66)
$X_4$	$-6.0 \pm 0.5$	-1.2 (0.15)	...	...	$-4.8 \pm 0.5$ (0.60)
$X_1$	$-3.3 \pm 0.4$	-1.0 (0.14)	...	...	$-2.3 \pm 0.4$ (0.32)
$X_3$	$-2.0 \pm 0.3$	-0.34 (0.15)	...	...	$-1.7 \pm 0.3$ (0.73)

TABLE II

Harmonic ( $\nu_{\tilde{q}j}^h$ ) and anharmonic ( $\nu_{\tilde{q}j}(0)$ ) phonon frequencies in units of THz and temperatures characteristic of the anharmonicity ( $\theta_{\tilde{q}j}$ ) in degrees K as obtained from Eqs (5) and (6).

mode	$\Gamma'_{25}$	$L'_3$	$L_1$	$L'_2$	$L_3$	$X_4$	$X_1$	$X_3$
$\nu_{\tilde{q}j}^h$	$9.181 \pm 0.009$	$8.726 \pm 0.035$	$7.391 \pm 0.008$	$6.700 \pm 0.009$	$1.919 \pm 0.003$	$8.340 \pm 0.017$	$7.267 \pm 0.013$	$2.431 \pm 0.007$
$\nu_{\tilde{q}j}(0)$	$9.120 \pm 0.009$	$8.673 \pm 0.035$	$7.343 \pm 0.008$	$6.668 \pm 0.009$	$1.899 \pm 0.003$	$8.270 \pm 0.017$	$7.223 \pm 0.013$	$2.407 \pm 0.007$
$\theta_{\tilde{q}j}$	$-18500 \pm 900$	$-20300 \pm 3200$	$-18900 \pm 800$	$-25400 \pm 1800$	$-12300 \pm 500$	$-14500 \pm 900$	$-20200 \pm 2000$	$-12400 \pm 700$

FIGURE CAPTIONS

Fig 1 Phonon frequencies vs temperature as obtained by the present authors (filled circles), Payne [1] (filled triangles), Zavaritskii [2] (crosses) and Brockhouse and Dasannacharya [5] (filled squares). The errors quoted by Payne do not exceed the size of any of the filled triangles. Brockhouse and Dasannacharya listed no errors and their results are shown only when they lie within the frames of the figures. The dashed-dotted and the dotted curves represent the mean results of Raman scattering experiments by Cerdeira and Cardona [11] and by Ray et al. [12], respectively. The open circles mark the results of a calculation by Cowley [7] when normalized to 9.01 THz at 300 K. The dashed curves represent the frequency variations as predicted by a quasiharmonic approximation [14] when normalized to the present data at 80 K (see Sec III B). The solid curves were obtained by least-squares fits of Eq (5) to the present data.

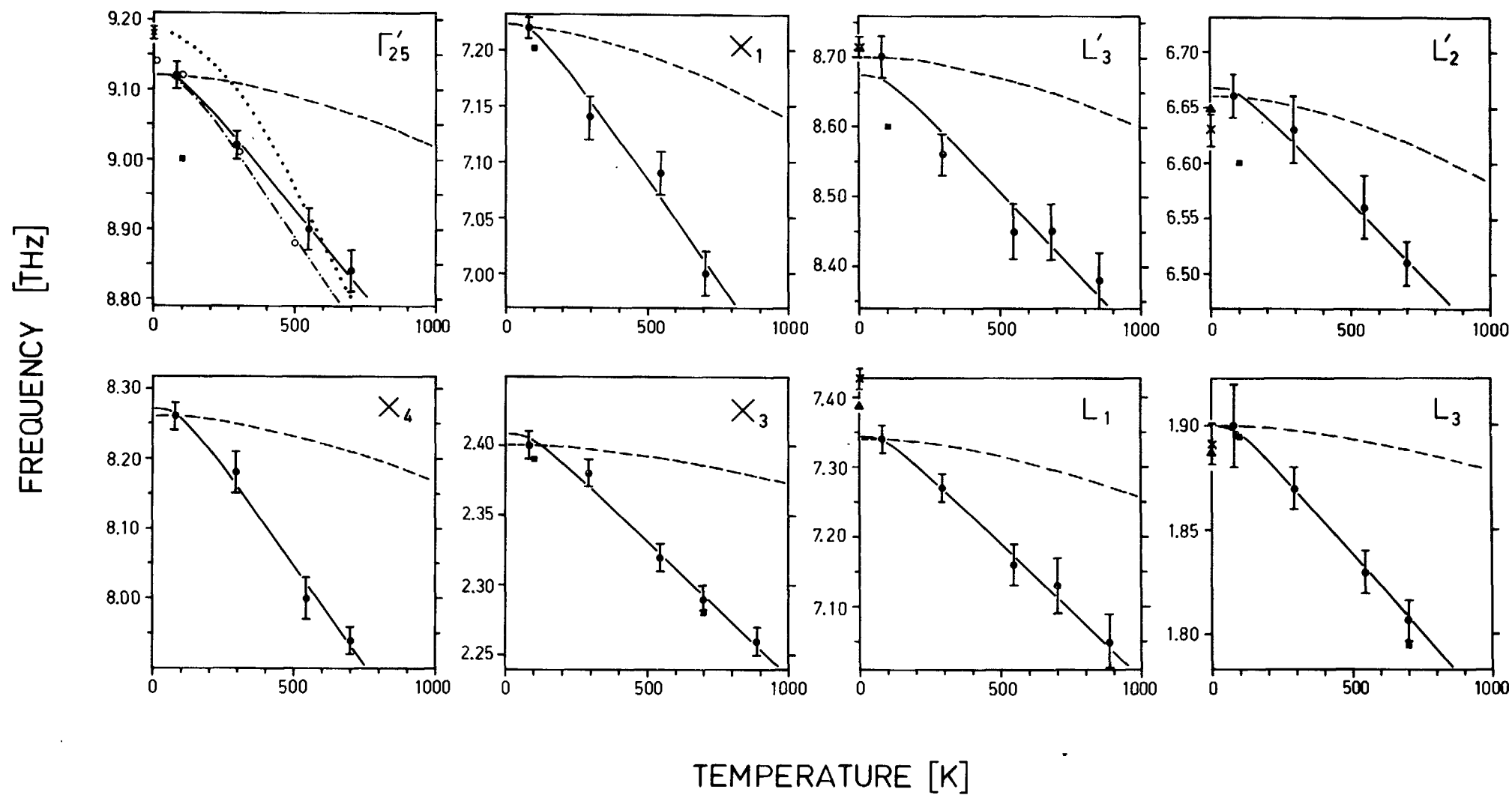
Fig 2 (a) Specific heat at constant pressure,  $C_P$ , of germanium as obtained by Flubacher et al. [21] (filled circles), Piesbergen [26] (open circles), Smith [28] (crosses), Greiner [27] (open square) and Gerlich et al. [29] (filled triangles). The dotted curve represents the mean of the results obtained by Chen and Turnbull [25] and the bars indicate the maximum scattering of points. The curves labeled  $C_P$  and  $C_V^h$  show the results of calculations from the present data as described in Sec III D. The arrow marks the value of the constant of Dulong and Petit.

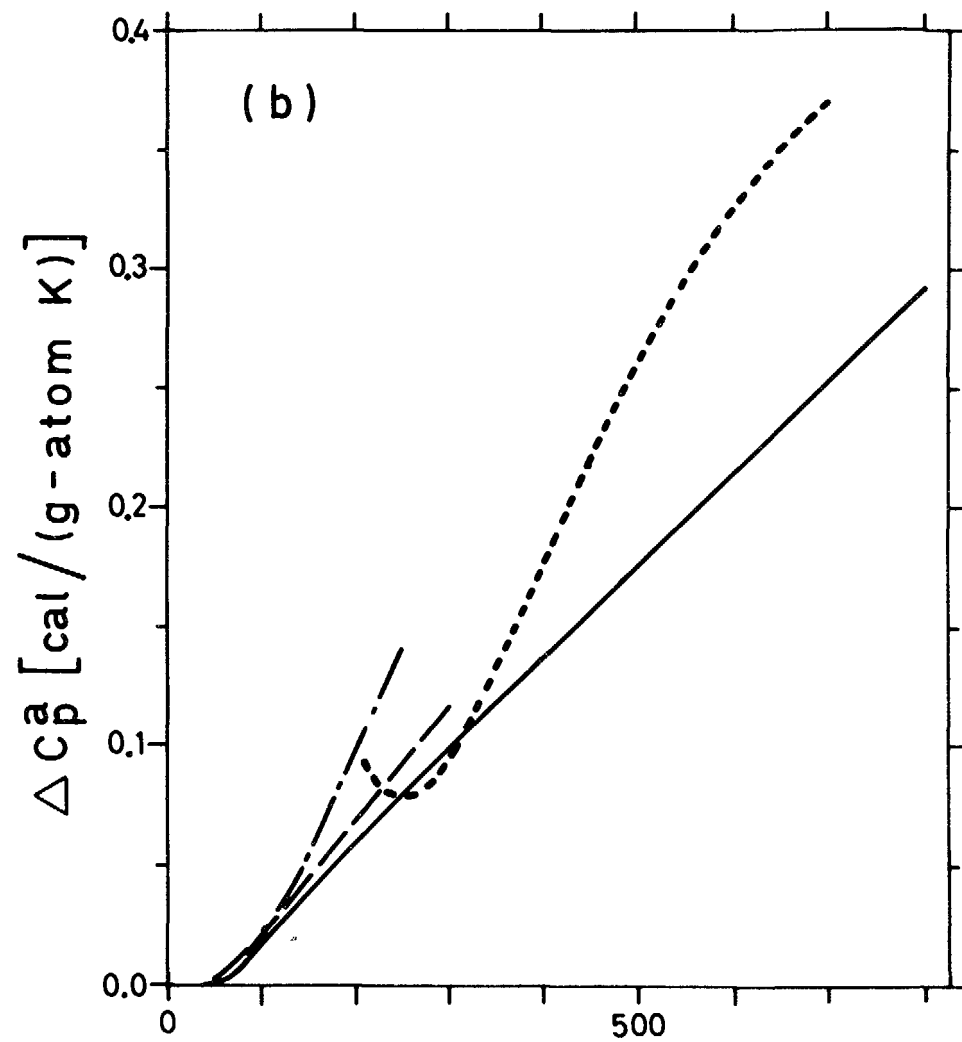
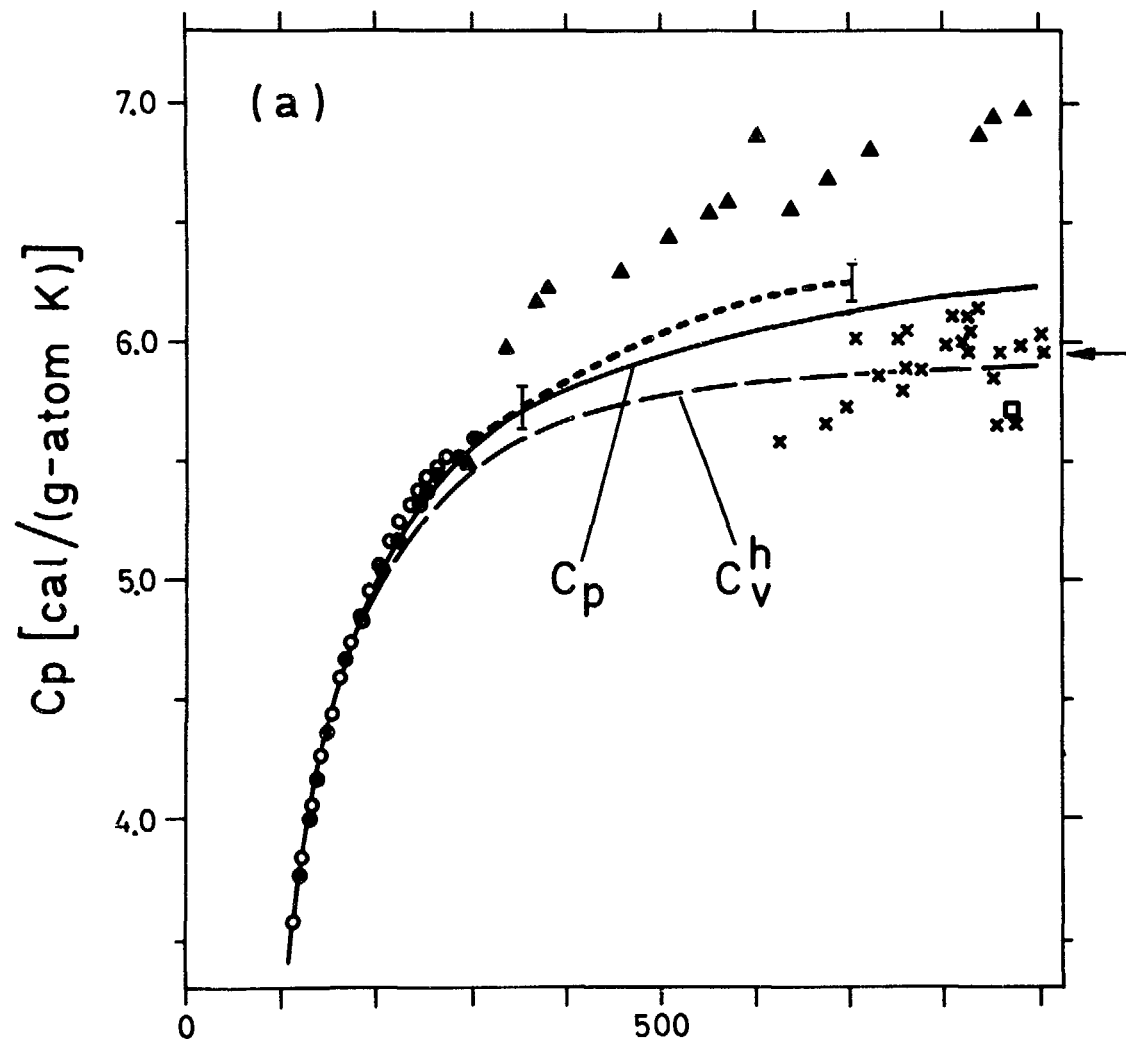
(b) The differences between three of the data sets in (a) and  $C_V^h$ , namely for Flubacher et al. (dashed curve), Piesbergen (dashed-dotted curve) and Chen and Turnbull (dotted curve). The solid curve represents  $C_P - C_V^h$  of the present calculation.

Fig 3 Phonon dispersion relations in germanium at 80 K. The symbols  $q_i$  are explained in Sec IV.

Fig 4 The velocities of the phonon modes of the high symmetry directions in germanium at 80 K as obtained by calculating the linear frequency gradients between both nearest and next-nearest points. (This means that the phonon velocity at  $\Gamma$  equals the velocity of sound divided by  $2\pi$ .) All published data [3] have been utilized. The error bars mark the root-mean-squares of the experimental errors and the filled squares indicate the velocities of the acoustic modes in the long-wave-length limit as calculated from the elastic constants [17]. The solid curves and the symbols  $q_i$  are explained in Sec IV.

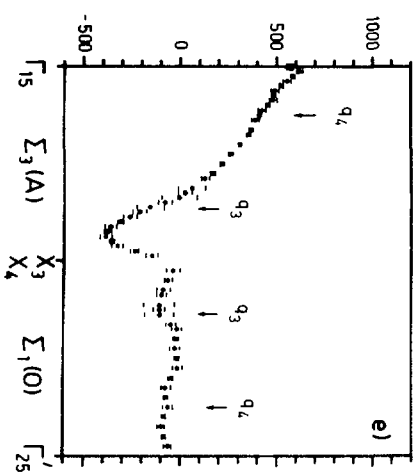
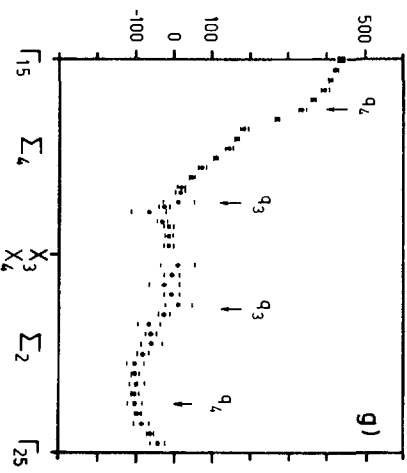
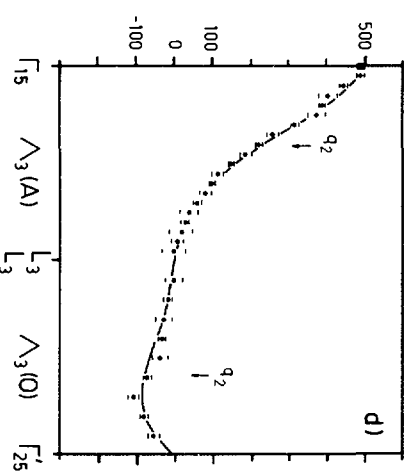
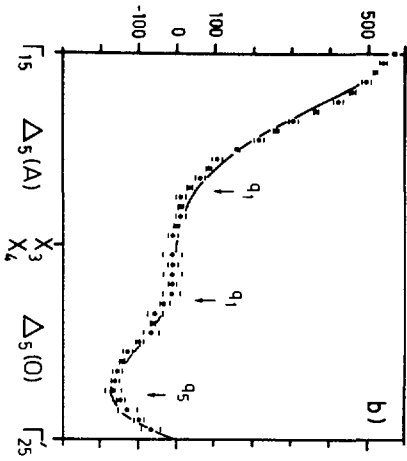
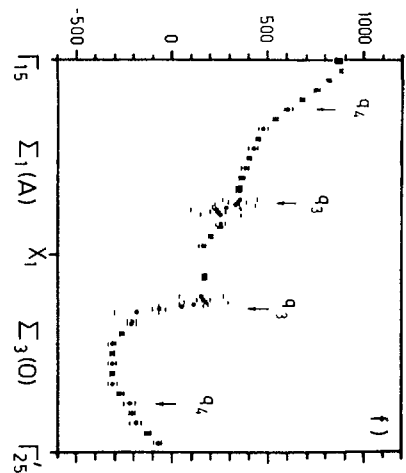
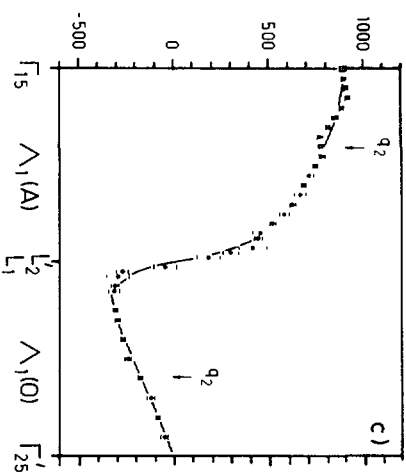
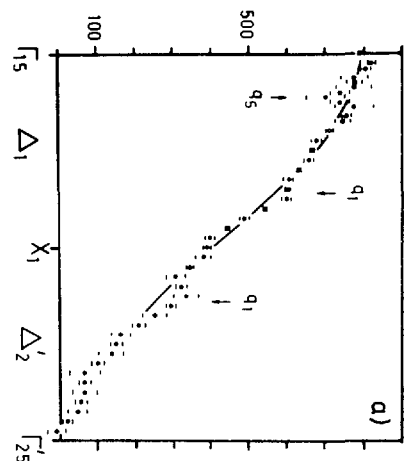








# PHONON VELOCITY [msec<sup>-1</sup>]





LIST OF PUBLISHED AE-REPORTS

1-420 (See back cover earlier reports.)

421. Decay curves and half-lives of gamma-emitting states from a study of prompt fission gamma radiation. By H. Albinsson. 1971. 28 p. Sw. cr. 15:-.

422. Adjustment of neutron cross section data by a least square fit of calculated quantities to experimental results. Part 1. Theory. By H. Häggblom. 1971. 28 p. Sw. cr. 15:-.

423. Personnel dosimetry at AB Atomenergi during 1969. By J. Carlsson and T. Wahlberg. 1971. 10 p. Sw. cr. 15:-.

424. Some elements of equilibrium diagrams for systems of iron with water above 100°C and with simple chloride, carbonate and sulfate melts. By D. Lewis. 1971. 40 p. Sw. cr. 15:-.

425. A study of material buckling in uranium-loaded assemblies of the fast reactor FR0. By R. Håkansson and L. I. Tirén. 1971. 32 p. Sw. cr. 15:-.

426. Dislocation line tensions in the noble metals, the alkali metals and  $\beta$ -Brass. By B. Pettersson and K. Malén. 1971. 14 p. Sw. cr. 15:-.

427. Studies of fine structure in the flux distribution due to the heterogeneity in some FR0 cores. By T. L. Andersson and H. Häggblom. 1971. 32 p. Sw. cr. 15:-.

428. Integral measurement of fission-product reactivity worths in some fast reactor spectra. By T. L. Andersson. 1971. 36 p. Sw. cr. 15:-.

429. Neutron energy spectra from neutron induced fission of  $^{235}\text{U}$  at 0.95 MeV and of  $^{238}\text{U}$  at 1.35 and 2.02 MeV. By E. Almén, B. Holmqvist and T. Wiedling. 1971. 16 p. Sw. cr. 15:-.

430. Optical model analyses of experimental fast neutron elastic scattering data. By B. Holmqvist and T. Wiedling. 1971. 238 p. Sw. cr. 20:-.

431. Theoretical studies of aqueous systems above 25°C. 1. Fundamental concepts for equilibrium diagrams and some general features of the water system. By Derek Lewis. 1971. 27 p. Sw. cr. 15:-.

432. Theoretical studies of aqueous systems above 25°C. 2. The iron - water system. By Derek Lewis. 1971. 41 p. Sw. cr. 15:-.

433. A detector for  $(n,\gamma)$  cross section measurements. By J. Hellström and S. Beshai. 1971. 22 p. Sw. cr. 15:-.

434. Influence of elastic anisotropy on extended dislocation nodes. By B. Pettersson. 1971. 27 p. Sw. cr. 15:-.

435. Lattice dynamics of CsBr. By S. Rolandson and G. Raunio. 1971. 24 p. Sw. cr. 15:-.

436. The hydrolysis of iron (III) and iron (II) ions between 25°C and 375°C. By Derek Lewis. 1971. 16 p. Sw. cr. 15:-.

437. Studies of the tendency of intergranular corrosion cracking of austenitic Fe-Cr-Ni alloys in high purity water at 300°C. By W. Hübner, B. Johansson and M. de Pourbaix. 1971. 30 p. Sw. cr. 15:-.

438. Studies concerning water-surface deposits in recovery boilers. By O. Strandberg, J. Arvesen and L. Dahl. 1971. 132 p. Sw. cr. 15:-.

439. Adjustment of neutron cross section data by a least square fit of calculated quantities to experimental results. Part II. Numerical results. By H. Häggblom. 1971. 70 p. Sw. cr. 15:-.

440. Self-powered neutron and gamma detectors for in-core measurements. By O. Strindehag. 1971. 16 p. Sw. cr. 15:-.

441. Neutron capture gamma ray cross sections for Ta, Ag, In and Au between 30 and 175 keV. By J. Hellström and S. Beshai. 1971. 30 p. Sw. cr. 15:-.

442. Thermodynamical properties of the solidified rare gases. By I. Ebbsjö. 1971. 46 p. Sw. cr. 15:-.

443. Fast neutron radiative capture cross sections for some important standards from 30 keV to 1.5 MeV. By J. Hellström. 1971. 22 p. Sw. cr. 15:-.

444. A Ge (Li) bore hole probe for in situ gamma ray spectrometry. By A. Lauber and O. Landström. 1971. 26 p. Sw. cr. 15:-.

445. Neutron inelastic scattering study of liquid argon. By K. Sköld, J. M. Rowe, G. Ostrowski and P. D. Randolph. 1972. 62 p. Sw. cr. 15:-.

446. Personnel dosimetry at Studsvik during 1970. By L. Hedlin and C.-O. Widell. 1972. 8 p. Sw. cr. 15:-.

447. On the action of a rotating magnetic field on a conducting liquid. By E. Dahlberg. 1972. 60 p. Sw. cr. 15:-.

448. Low grade heat from thermal electricity production. Quantity, worth and possible utilisation in Sweden. By J. Christensen. 1972. 102 p. Sw. cr. 15:-.

449. Personnel dosimetry at studsvik during 1971. By L. Hedlin and C.-O. Widell. 1972. 8 p. Sw. cr. 15:-.

450. Deposition of aerosol particles in electrically charged membrane filters. By L. Ström. 1972. 60 p. Sw. cr. 15:-.

451. Depth distribution studies of carbon in steel surfaces by means of charged particle activation analysis with an account of heat and diffusion effects in the sample. By D. Brune, J. Lorenzen and E. Witalis. 1972. 46 p. Sw. cr. 15:-.

452. Fast neutron elastic scattering experiments. By M. Salama. 1972. 98 p. Sw. cr. 15:-.

453. Progress report 1971 Nuclear chemistry. 1972. 21 p. Sw. cr. 15:-.

454. Measurement of bone mineral content using radiation sources. An annotated bibliography. By P. Schmeling. 1972. 64 p. Sw. cr. 15:-.

454. Measurement of bone mineral content using radiation sources. An annotated bibliography. Suppl. 1. By P. Schmeling. 1974. 26 p. Sw. cr. 20:-.

455. Long-term test of self-powered detectors in HBWR. By M. Brakas, O. Strindehag and B. Söderlund. 24 p. 1972. Sw. cr. 15:-.

456. Measurement of the effective delayed neutron fraction in three different FR0-cores. By L. Moberg and J. Kockum. 1972. Sw. cr. 15:-.

457. Applications of magnetohydrodynamics in the metal industry. By T. Robinson, J. Braun and S. Linder. 1972. 42 p. Sw. cr. 15:-.

458. Accuracy and precision studies of a radiochemical multielement method for activation analysis in the field of life sciences. By K. Samsahl. 1972. 20 p. Sw. cr. 15:-.

459. Temperature increments from deposits on heat transfer surfaces: the thermal resistivity and thermal conductivity of deposits of magnetite, calcium hydroxy apatite, humus and copper oxides. By T. Kelén and J. Arvesen. 1972. 69 p. Sw. cr. 15:-.

460. Ionization of a high-pressure gas flow in a longitudinal discharge. By S. Palmgren. 1972. 20 p. Sw. cr. 15:-.

461. The caustic stress corrosion cracking of alloyed steels - an electrochemical study. By L. Dahl, T. Dahlgren and N. Lagmyr. 1972. 43 p. Sw. cr. 15:-.

462. Electrodeposition of "point"  $\text{Cu}^{2+}$  roentgen sources. By P. Beronius, B. Johansson and R. Söremark. 1972. 12 p. Sw. cr. 15:-.

463. A twin large-area proportional flow counter for the assay of plutonium in human lungs. By R. C. Sharma, I. Nilsson and L. Lindgren. 1972. 50 p. Sw. cr. 15:-.

464. Measurements and analysis of gamma heating in the R2 core. By R. Carlsson and L. G. Larsson. 1972. 34 p. Sw. cr. 15:-.

465. Determination of oxygen in zirconium surfaces by means of charged particle activation analysis. By J. Lorenzen and D. Brune. 1972. 18 p. Sw. cr. 15:-.

466. Neutron activation of liquid samples at low temperature in reactors with reference to nuclear chemistry. By D. Brune. 1972. 8 p. Sw. cr. 15:-.

467. Irradiation facilities for coated particle fuel testing in the Studsvik R2 reactor. By S. Sandklef. 1973. 28 p. Sw. cr. 20:-.

468. Neutron absorber techniques developed in the Studsvik R2 reactor. By R. Bodh and S. Sandklef. 1973. 26 p. Sw. cr. 20:-.

469. A radiochemical machine for the analysis of Cd, Cr, Cu, Mo and Zn. By K. Samsahl, P. O. Wester, G. Blomqvist. 1973. 13 p. Sw. cr. 20:-.

470. Proton pulse radiolysis. By H. C. Christensen, G. Nilsson, T. Reitberger and K.-Å. Thuomas. 1973. 26 p. Sw. cr. 20:-.

471. Progress report 1972. Nuclear chemistry. 1973. 28 p. Sw. cr. 20:-.

472. An automatic sampling station for fission gas analysis. By S. Sandklef and P. Svensson. 1973. 52 p. Sw. cr. 20:-.

473. Selective step scanning: a simple means of automating the Philips diffractometer for studies of line profiles and residual stress. By A. Brown and S. A. Lindh. 1973. 38 p. Sw. cr. 20:-.

474. Radiation damage in  $\text{CaF}_2$  and  $\text{BaF}_2$  investigated by the channeling technique. By R. Hellborg and G. Skog. 1973. 38 p. Sw. cr. 20:-.

475. A survey of applied instrument systems for use with light water reactor containments. By H. Tuxen-Meyer. 1973. 20 p. Sw. cr. 20:-.

476. Excitation functions for charged particle induced reactions in light elements at low projectile energies. By J. Lorenzen and D. Brune. 1973. 154 p. Sw. cr. 20:-.

477. Studies of redox equilibria at elevated temperatures 3. Oxide/oxide and oxide/metal couples of iron, nickel, copper, silver, mercury and antimony in aqueous systems up to 100°C. By Karin Johansson, Kerstin Johansson and Derek Lewis. 1973. 42 p. Sw. cr. 20:-.

478. Irradiation facilities for LWR fuel testing in the Studsvik R2 reactor. By S. Sandklef and H. Tomani. 1973. 30 p. Sw. cr. 20:-.

479. Systematics in the  $(p,xn)$  and  $(p,pxn)$  reaction cross sections. By L. Jéki. 1973. 14 p. Sw. cr. 20:-.

480. Axial and transverse momentum balance in subchannel analysis. By S. Z. Rouhani. 1973. 58 p. Sw. cr. 20:-.

481. Neutron inelastic scattering cross sections in the energy range 2 to 4.5 MeV. Measurements and calculations. By M. A. Etemad. 1973. 62 p. Sw. cr. 20:-.

482. Neutron elastic scattering measurements at 7.0 MeV. By M. A. Etemad. 1973. 28 p. Sw. cr. 20:-.

483. Zooplankton in Tvären 1961-1963. By E. Almqvist. 1973. 50 p. Sw. cr. 20:-.

484. Neutron radiography at the Studsvik R2-0 reactor. By I. Gustafsson and E. Sokolowski. 1974. 54 p. Sw. cr. 20:-.

485. Optical model calculations of fast neutron elastic scattering cross sections for some reactor materials. By M. A. Etemad. 1974. 165 p. Sw. cr. 20:-.

486. High cycle fatigue crack growth of two zirconium alloys. By V. S. Rao. 1974. 30 p. Sw. cr. 20:-.

487. Studies of turbulent flow parallel to a rod bundle of triangular array. By B. Kjellström. 1974. 190 p. Sw. cr. 20:-.

488. A critical analysis of the ring expansion test on zirconium cladding tubes. By K. Pettersson. 1974. 8 p. Sw. cr. 20:-.

489. Bone mineral determinations. Proceedings of the symposium on bone mineral determinations held in Stockholm-Studsvik, Sweden, 27-29 May 1974. Vol. 3. Bibliography on bone morphology and densitometry in man. By A. Horsman and M. Simpson. 1974. 112 p. Sw. cr. 20:-.

490. The over-power ramp fuel failure phenomenon and its burn-up dependence - need of systematic, relevant and accurate irradiation investigations. - Program proposal. By Hilding Mogard. 1974. Sw. cr. 20:-.

491. Phonon Anharmonicity of Germanium in the Temperature Range 80-880 K. By G. Nelin and G. Nilsson. 1974. 28 p. Sw. cr. 20:-.

List of published AES-reports (In Swedish)

1. Analysis by means of gamma spectrometry. By D. Brune. 1961. 10 p. Sw. cr. 6:-.
2. Irradiation changes and neutron atmosphere in reactor pressure vessels - some points of view. By M. Grounes. 1962. 33 p. Sw. cr. 6:-.
3. Study of the elongation limit in mild steel. By G. Östberg and R. Attermo. 1963. 17 p. Sw. cr. 6:-.
4. Technical purchasing in the reactor field. By Erik Jonson. 1963. 64 p. Sw. cr. 8:-.
5. Ågesta nuclear power station. Summary of technical data, descriptions, etc. for the reactor. By B. Lilliehöök. 1964. 336 p. Sw. cr. 15:-.
6. Atom Day 1965. Summary of lectures and discussions. By S. Sandström. 1966. 321 p. Sw. cr. 15:-.
7. Building materials containing radium considered from the radiation protection point of view. By Stig O. W. Bergström and Tor Wahlberg. 1967. 26 p. Sw. cr. 10:-.
8. Uranium market. 1971. 30 p. Sw. cr. 15:-.
9. Radiography day at Studsvik. Tuesday 27 april 1971. Arranged by AB Atomenergi, IVA's Committee for nondestructive testing and TRC AB. 1971. 102 p. Sw. cr. 15:-.
10. The supply of enriched uranium. By M. Mårtensson. 1972. 53 p. Sw. cr. 15:-.
11. Fire studies of plastic-insulated electric cables, sealing lead-in wires and switch gear cubicles and floors. 1973. 117 p. Sw. cr. 35:-.

Additional copies available from the Library of AB Atomenergi, Fack, S-611 01 Nyköping 1, Sweden.